ACS APPLIED MATERIALS & INTERFACES

Research Article

www.acsami.org

Enhanced Li Storage Performance of $LiNi_{0.5}Mn_{1.5}O_4$–Coated $0.4Li_2MnO_3{\cdot}0.6LiNi_{1/3}Co_{1/3}Mn_{1/3}O_2$ Cathode Materials for Li-Ion Batteries

Yufang Chen,[†] Kai Xie,[†] Chunman Zheng,*[,†] Zhongyun Ma,[†] and Zhongxue Chen*[,†,‡]

[†]College of Aerospace Science and Engineering, National University of Defense Technology, Changsha, Hunan 410073, China

[‡]College of Chemistry and Chemical Engineering, Hunan University, Changsha, Hunan 410082, China

ABSTRACT: In this study, Li-rich cathode, $0.4Li_2MnO_3{\cdot}0.6LiNi_{1/3}Co_{1/3}Mn_{1/3}O_2$ was synthesized by a resorcinol formaldehyde assisted sol–gel method for the first time. Then, the surface of the as-prepared Li-rich cathode was modified with different amounts of $LiNi_{0.5}Mn_{1.5}O_4$ (5, 10, and 20 wt %) through a simple dip-dry approach. The structural and electrochemical characterizations revealed that the spinel $LiNi_{0.5}Mn_{1.5}O_4$ coating not only can prevent electrolytes from eroding the Li-rich core but also can facilitate fast lithium ion transportation. As a result, the 20 wt % coated sample delivered an initial discharge capacity of 298.6 mAh g^{-1} with a Coulombic efficiency of 84.8%, compared to 281.1 mAh g^{-1} and 70.2%, respectively, for the bare sample. Particularly, the coated sample demonstrates a Li storage capacity of 170.7 mAh g^{-1} and capacity retention of 94.4% after 100 cycles at a high rate of 5 C (1250 mA g^{-1}), showing a prospect for practical lithium battery applications. More significantly, the synthetic method proposed in this work is facile and low-cost and possibly could be adopted for large-scale production of surface-modified cathode materials.

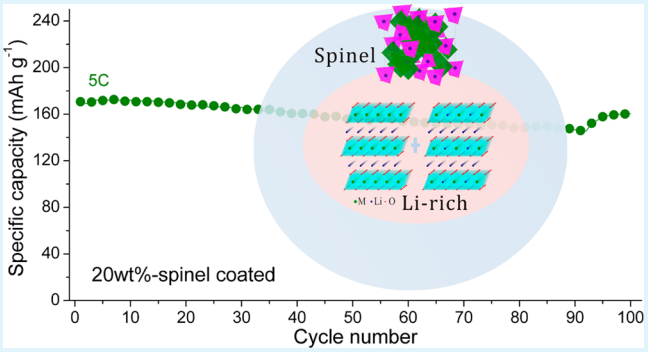

KEYWORDS: *Li-rich cathode, surface modification, spinel, Li storage, rate capability*

1. INTRODUCTION

Recenlty, many Li compounds, including high-voltage spinels, silicates, and Ni-rich layered materials, were investigated to substitute traditional cathodes for next generation Li-ion batteries.[1−4] Among them, layered lithium-rich materials, $xLi_2MnO_3{\cdot}(1-x)$ $LiMO_2$, attracted more attention due to their favorable features such as high capacity (>250 mAh g^{-1}), low cost, and good safety.[5] However, the commercial application of Li-rich cathode is hindered by several drawbacks, including the intrinsic low electrical conductivity, dissolution of Mn in electrolytes, and structure transformation during cycling.[6−8] These lead to rapid capacity loss, low Coulombic efficiency, and poor cycling performance.

To solve these problems, many strategies have been proposed to tailor the structures and morphologies of the Li-rich materials through ion-doping,[9] nanoarchitecture,[10−14] or surface modification.[15−21] Among the above-mentioned approaches, surface modification is researched mostly due to its effectivity and simplicity. Hence, many inorganic compounds, such as oxides, fluorides, and phosphates, were explored as the coating layer to stabilize the surface structure. However, these coatings will lower the whole specific capacity and have limited contribution to fast lithium ion transport of the Li-rich cathode. Recently, Wu et al.[22] constructed a spinel/layered heterostructure by encapsulating layered lithium-rich material with a nanospinel mixture $LiNi_xMn_{2-x}O_4$, and this composite material exhibited outstanding rate performance, delivering a discharge capacity of ∼180 mAh g^{-1} at 10 C. Actually, different coating spinel content may largely affect the specific capacity, cycling stability, and the rate capability of Li-rich cathode. Therefore, it is necessary to further investigate the effect of a spinel coating layer on the electrochemical performance of Li-rich layered oxides.

In this study, nanosized $0.4Li_2MnO_3{\cdot}0.6LiNi_{1/3}Co_{1/3}Mn_{1/3}O_2$ was first synthesized by a resorcinol formaldehyde assisted sol–gel method, and spinel coating was subsequently performed through a simple dip-dry approach. Compared with the bare sample, the $LiNi_{0.5}Mn_{1.5}O_4$ coated $0.4Li_2MnO_3{\cdot}0.6LiNi_{1/3}Co_{1/3}Mn_{1/3}O_2$ shows significantly improved Coulombic efficiency and rate capability. The effect of a spinel coating layer on the electrochemical performance of Li-rich cathode was also discussed in detail.

2. EXPERIMENTAL SECTION

2.1. Materials Preparation. $0.4Li_2MnO_3{\cdot}0.6LiNi_{1/3}Co_{1/3}Mn_{1/3}O_2$ was synthesized with a resorcinol formaldehyde assisted sol–gel method. Resorcinol, formaldehyde, $LiCOOCH_3{\cdot}2H_2O$, Ni-

Received: July 7, 2014
Accepted: September 16, 2014
Published: September 16, 2014

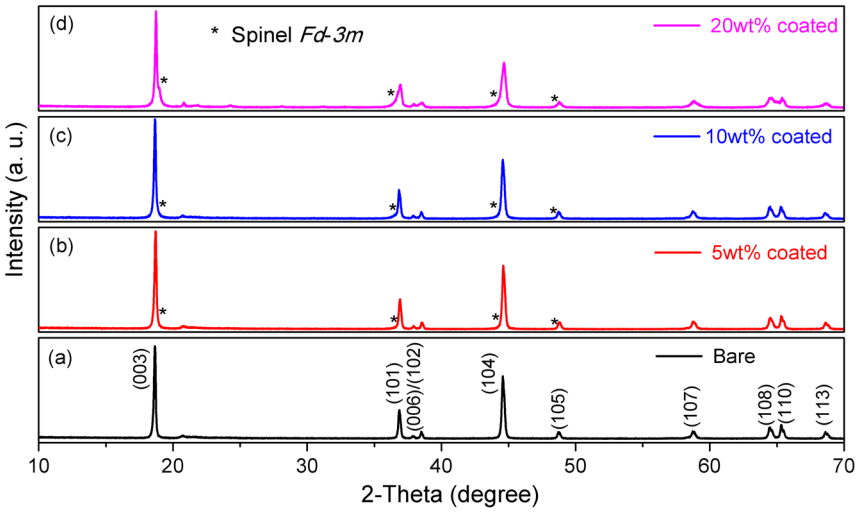

Figure 1. XRD patterns of the (a) bare sample and the (b) 5, (c) 10, and (d) 20 wt % coated samples.

$(COOCH_3)_2{\cdot}4H_2O$, $Co(COOCH_3)_2{\cdot}4H_2O$, and $Mn(COOCH_3)_2{\cdot}4H_2O$ was dissolved in distilled water at the required stoichiometry. After being stirred thoroughly, the solution was heated at 60 °C until a viscous liquid formed, and then it was dried at 90 °C for 12 h. The resulting solid was calcined at 900 °C for 12 h to obtain Li-rich layered oxides.

Spinel coating was subsequently performed through a dip-dry approach. The as-prepared $0.4Li_2MnO_3{\cdot}0.6LiNi_{1/3}Co_{1/3}Mn_{1/3}O_2$ was dispersed in ethanol by ultrasonic treatment. The suspension was stirred vigorously as the required amounts of $LiCOOCH_3{\cdot}2H_2O$, $Ni(COOCH_3)_2{\cdot}4H_2O$, and $Mn(COOCH_3)_2{\cdot}4H_2O$ were added, and then the suspension was heated at 80 °C until all the liquid evaporated. The resulting solid was calcined at 500 °C for 5 h to obtain the final coated sample. Herein, the coated spinel contents were controlled at 5, 10, and 20 wt %.

2.2. Morphology and Structure Characterizations. X-ray diffraction (XRD) characterization was performed with a high-power X-ray diffractometer. The morphologies of the bare and coated samples were investigated with scanning electron microscopy (SEM, Histachi S-4800) and transmission electron microscopy (TEM, JEM-2100F).

2.3. Electrochemical Measurements. The electrochemical measurements of the cathode materials were performed using 2016-type coin cells with lithium foil as a counter electrode. The electrolyte was 1.2 M $LiPF_6$ dissolved in a mixture of ethylene carbonate (EC) and diethyl carbonate (DEC) (3:7 w/w). Cathodes were prepared by mixing cathode materials, super P and poly vinylidene fluoride (PVDF) in *N*-methyl pyrrolidone (NMP) solution with weight ratio of 8:1:1. The slurry was cast onto an Al foil and was then dried overnight in a vacuum oven at 80 °C. The coin cells were cycled galvanostatically in the voltage range of 4.8–2.0 V at room temperature. Cyclic voltammetric measurements were carried out at the scan rate of 0.1 mV s^{-1}. Electrochemical impedance spectra (EIS) measurements were conducted in the frequency range of 100 kHz to 0.01 Hz.

3. RESULTS AND DISCUSSION

XRD patterns of the pristine $0.4Li_2MnO_3{\cdot}0.6LiNi_{1/3}Co_{1/3}Mn_{1/3}O_2$ and all coated samples are shown in Figure 1. Clearly, all the peaks of the bare sample can be indexed to the layered structure ($R\bar{3}m$), except for the weak superlattice reflections observed between 20 and 25°, which are due to the monoclinic ($C2/m$) structure. Compared with the bare sample, all the coated samples have similar XRD patterns, but the peaks at 18.7, 36.8, 44.6, and 48.8° display obvious broadening and asymmetry. It is evident that these peaks are composed of two types of XRD patterns, including layered structure and spinel $LiNi_{0.5}Mn_{1.5}O_4$ ($Fd\bar{3}m$); the spinel phase did not show a high degree of crystallinity due to the low calcined temperature (500 °C). It is interestingly noted that the tendency of peak broadening and asymmetry increases as the coating content of spinel increases.

To further study the influence of coating spinel on the crystalline structure of Li-rich materials, we also calculated the lattice parameters, c/a and $I_{(003)}/I_{(104)}$, of the four samples. As presented in Table 1, both lattice parameters and c/a values of

Table 1. Lattice Parameters ($R\bar{3}m$), c/a, and $I_{(003)}/I_{(104)}$ for Bare and Coated Samples

sample	a (Å)	c (Å)	c/a	$I_{(003)}/I_{(104)}$
bare	2.8498	14.2142	4.987	1.478
5% coated	2.8508	14.2151	4.986	1.535
10% coated	2.8515	14.2113	4.983	1.682
20% coated	2.8514	14.2122	4.984	1.978

the four samples remained almost unchanged, indicating the coating spinel did not affect the crystallinity of the layered structure. Generally, the ratio of $I_{(003)}/I_{(104)}$ in the XRD patterns can be used to evaluate the degree of cation mixing in the Li-layers of these materials. The ratio of $I_{(003)}/I_{(104)}$ is 1.478 for the bare sample, which is larger than 1.2, suggesting that the cation disorder in the Li-layers can be ignored. In addition, we can find that the ratio of $I_{(003)}/I_{(104)}$ increases as the coating spinel content increases, but this trend did not mean that the coated sample has a better layered structure. Actually, the (003) and (104) peaks of the layered structure overlap with the (111) and (400) peaks of spinel $LiNi_{0.5}Mn_{1.5}O_4$, respectively, and the ratio of $I_{(111)}/I_{(400)}$ in spinel is larger than 2.0. As a result, the ratio of $I_{(003)}/I_{(104)}$ in the layered structure gradually increases along with spinel coating content.

Figure 2 shows the SEM images of the bare and coated samples. The image in Figure 2a reveals that the bare sample is composed of uniformly distributed polyhedral particles with diameters in a narrow range of ~200 nm, smooth facets, and sharp edges. When coated by spinel $LiNi_{0.5}Mn_{1.5}O_4$ (Figure 2b–d), the surface of the coated samples turned rougher and fuzzier, especially for the 20 wt % coated sample. This observation indicates that the surfaces of Li-rich particles are almost fully covered by $LiNi_{0.5}Mn_{1.5}O_4$ with low crystallinity.

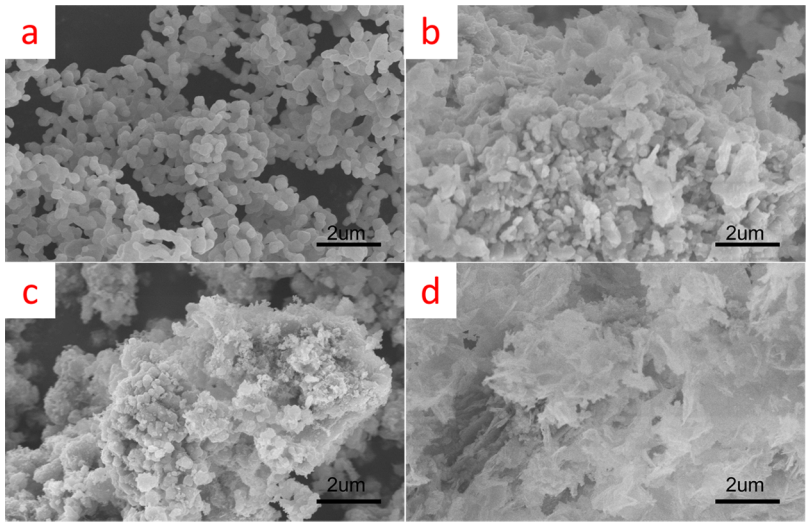

Figure 2. SEM images of the (a) bare sample and the (b) 5, (c) 10, and (d) 20 wt % coated samples.

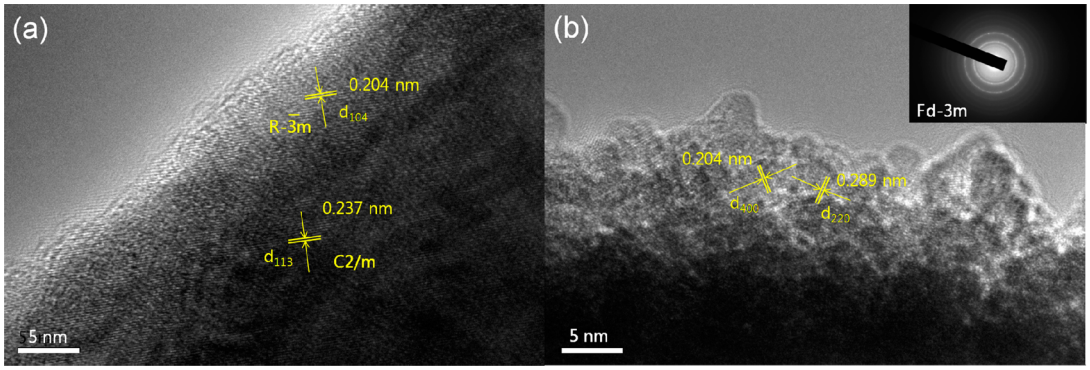

Figure 3. TEM images of the (a) bare sample and (b) 20 wt % coated sample.

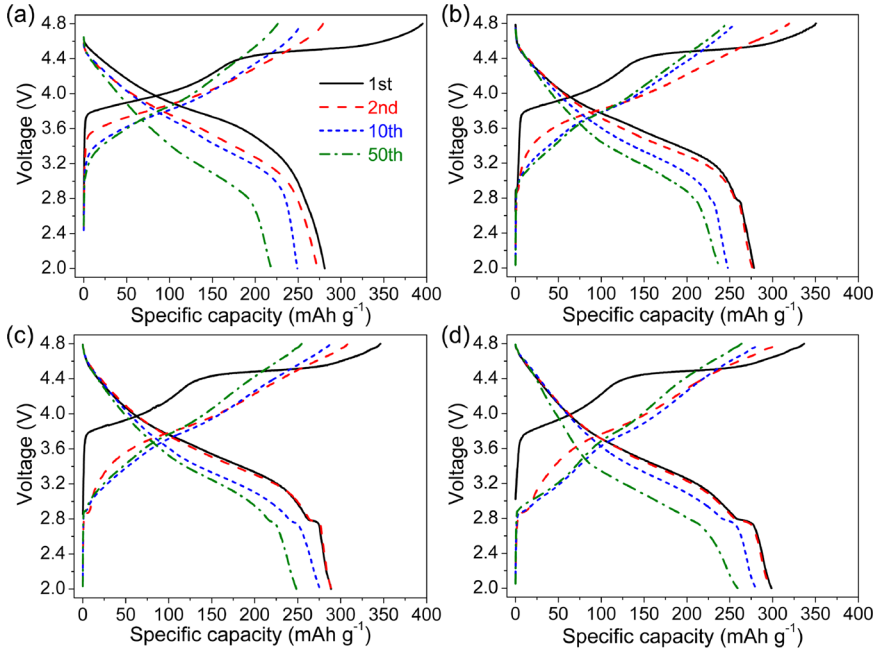

Figure 4. Charge/discharge curves of the (a) bare sample and the (b) 5, (c) 10, and (d) 20 wt % coated samples at C/20 (1 C = 250 mA g^{-1}).

To further confirm the effective coating of spinel on the surface of Li-rich particles, we also carried out high-resolution TEM characterizations for the bare and 20 wt % coated samples. In Figure 3a, two types of legible lattice fringes with basal distances of 2.04 and 2.37 Å can be detected, which can be indexed to the (104) plane of layered structure ($R\bar{3}m$) and

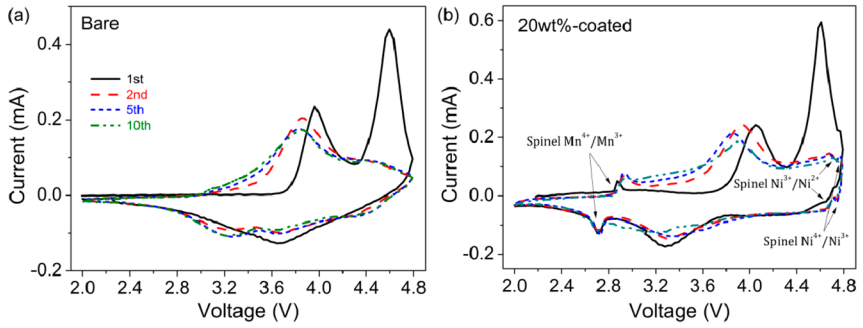

Figure 5. Cyclic voltammograms of the (a) bare and (b) 20 wt % coated samples.

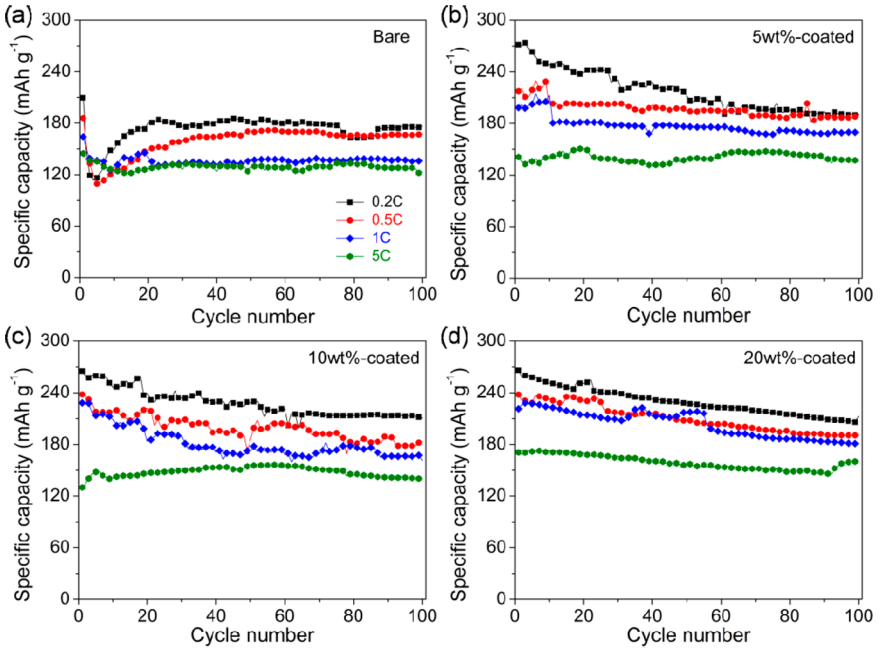

Figure 6. Discharge capacities of the bare and coated samples cycled at different cycling rates (1 C = 250 mA g^{-1}).

the (113) plane of monoclinic structure ($C2/m$). Obviously, it indicates that the bare sample is a solid solution with monoclinic symmetry and layered symmetry, which is consistent with many other reports[23,24] and our previous work.[25] Figure 3b directly shows the coating morphology of the 20 wt % coated sample; the lattice fringe distances of the coating layer were measured to be 2.04 and 2.89 Å, corresponding to the (400) and (220) planes of spinel $LiNi_{0.5}Mn_{1.5}O_4$ ($Fd3m$), respectively. It is also worth noting that the coating spinel $LiNi_{0.5}Mn_{1.5}O_4$ has relatively low crystallinity, which is indicated by the ED pattern shown in Figure 3b (inset). This observation is in good agreement with the XRD (Figure 1) and SEM (Figure 2) results.

Figure 4 shows the galvanostatic charge and discharge curves of the bare and coated samples at a current density of C/20 (1 C = 250 mA g^{-1}). As can be seen, the bare sample shows a representative profile of lithium-rich cathode, comprising two parts in the charge curve. The first part below 4.45 V originated from reversible lithium intercalation/deintercalation in layered structure, while the other one above 4.45 V should be attributed to the monoclinic Li_2MnO_3. Compared with the bare sample, the coated samples displayed almost the same charge/discharge curves except for the additional prolonged profiles in the voltage range of 4.8−4.6 V and 2.9−2.7 V during discharge, which can be attributed to the reduction of Ni^{4+} to Ni^{2+} and Mn^{4+} to Mn^{3+} in $LiNi_{0.5}Mn_{1.5}O_4$. The initial discharge capacities of the bare samples and the 5, 10, and 20 wt % coated samples are 281.1, 278.3, 288.8, and 298.6 mA h g^{-1}, respectively. Therefore, it can be calculated that the utilizations of the Li-rich components in the four samples are 84.4, 85.9, 90.8, and 99.4% (theoretic capacity, 333 mAh g^{-1}) if the capacity of spinel $LiNi_{0.5}Mn_{1.5}O_4$ is not counted, indicating that the coating spinel can help to enhance the discharge capacity of Li-rich core, which is probably due to maintaining lithium vacancies of the layered material by the coating spinel around 3.5 V. In addition, the initial Coulombic efficiencies of the 5, 10, and 20 wt % coated samples are 79.4, 83.2, and 84.8%. In contrast, the initial Coulombic efficiency of the bare sample is only 70.2%. This improvement demonstrates that the coating spinel can effectively protect the layered core from erosion of electrolytes and stabilize the surface structure. After the first cycle, the capacity and average discharge voltage of the bare sample dropped gradually, and it only delivered capacity of 218.6 mAh g^{-1} after 50 cycles, which should be attributed to the continuous structure transformation from layer to spinel. In contrast, the 5, 10, and 20 wt % coated samples could retain capacities of 238.3 mAh g^{-1}, 248.4 mAh g^{-1}, 259.2 mAh g^{-1} after 50 cycles. More importantly, the voltage decay for the

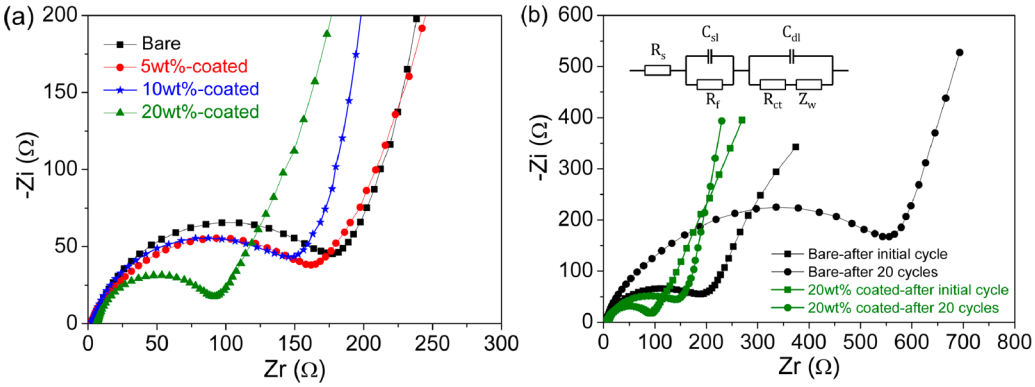

Figure 7. Electrochemical impedance spectra (EIS) of (a) the bare and coated samples before cycling and (b) the bare and 20 wt % coated samples after the 1st and 20th cycles in the frequency range of 100 kHz to 0.01 Hz.

coated samples is significantly less than the bare sample, further proving the positive effect on the surface structure stability of Li-rich materials by spinel coating.

The corresponding cathodic and anodic reactions occurring on the bare and coated samples could be identified in their cyclic voltammograms. Figure 5a presents typical CV curves of the Li-rich cathode. The main features of the material are two anodic peaks that appear at ~4.0 and ~4.6 V in the first positive scan, which correspond to the oxidation of M components (M = Ni^{2+}, Co^{3+}) and irreversible oxidation of O^{2-}, respectively. In the reverse negative scan, the cathodic peaks located at ~3.6 V are ascribed to the reduction of Ni^{4+} and Co^{4+}, the cathodic peak observed at ~3.3 V could be explained by the reduction of Mn^{4+} which balances the oxygen valence due to the loss of oxygen in the first charge.[26−29] Compared to the bare sample, the 20 wt % coated sample (Figure 5b) shows similar CV curves in the voltage range of 4.6−3.0 V, except for the three pairs of redox peaks centered in the high voltage range of 4.8−4.6 V and low voltage range of 3.0−2.6 V. These peaks correspond to the reversible reactions of the Ni^{3+}/Ni^{4+}, Ni^{2+}/Ni^{3+}, and Mn^{3+}/Mn^{4+} couples in the spinel $LiNi_{0.5}Mn_{1.5}O_4$, the symmetric shapes and areas indicate the structural stability of the coating spinel.[2,3]

The cycling performances of the bare and coated samples at different current densities are shown in Figure 6. The data are collected by charging at 0.2 C and discharging at various rates. As shown in Figure 6a, the bare sample delivered an initial capacity of 210 mAh g^{-1} at 0.2 C, but the capacity dropped suddenly in the second cycle. Nevertheless, as the cathode was wetted and activated,[30,31] the capacity rose gradually to 180 mAh g^{-1} after 20 cycles and subsequently remained stable. The same trend was also observed at the other rates for the bare sample, which can exhibit capacities of 167, 136, and 123 mAh g^{-1} at 0.5, 1, and 5 C, respectively, after 100 cycles. In contrast, the coated samples delivered gradually enhanced capacity at the same rates as the coating spinel content increases (Figure 6b−d) and did not undergo the activation process observed for the bare sample, which is probably because the coating spinel itself could preactivate Li-rich cathode and alter the initial electrochemical reaction before charging.[16,22,28,29] For instance, the 20 wt % coated sample (Figure 6d) can retain capacities of 213, 191, and 181 mAh g^{-1} at 0.2, 0.5, and 1C after 100 cycles. More significantly, the discharge capacity still can reach 161 mAh g^{-1} at a high rate of 5 C after 100 cycles, corresponding to capacity retention of 94.4%. Such superior rate capability and cycling performance would originate from the coating spinel, which not only can prevent electrolytes from eroding the Li-rich core but also can facilitate fast lithium ions transportation due its intrinsic three-dimensional (3D) Li^+ diffusing channels.

To gain further insight into the essence of improvement in high-rate capability, we conducted electrochemical impedance spectra (EIS) of the bare sample and the 5, 10, and 20 wt % coated samples. As shown in Figure 7a, all four Nyquist plots display a semicircle at high frequency and a sloped line at low-frequency, corresponding to the charge transfer resistance at electrolyte-electrode interfacial (R_{ct}) and the lithium diffusion Warburg impedance within the electrode, respectively.[16,25] By comparing the size of the arcs in Figure 7a, we found that the diameters of the semicircles gradually decrease as the coated amount increases, and the 20 wt % coated sample has the lowest resistance of all the four samples, suggesting that the spinel coating can accelerate surface charge transfer and the lithium-ion diffusion processes. In addition, compared to the sample before cycling, the EIS spectra of the 20 wt % coated sample after the initial cycle (Figure 7b) show almost identical impedance semicircles. In comparison, the bare sample revealed an obvious increase in its impedance semicircles after initial cycle. Moreover, the resistance of the bare sample increased largely after 20 cycles, while the resistance of the 20 wt % coated sample changed just a little. These comparisons further demonstrate that the coating spinel can effectively guarantee the stability of the surface structure, ensuring superior cycling performance.

4. CONCLUSION

In summary, we have successfully prepared $LiNi_{0.5}Mn_{1.5}O_4$-coated $0.4Li_2MnO_3{\cdot}0.6LiNi_{1/3}Co_{1/3}Mn_{1/3}O_2$ by a simple dip-dry method. The structures and electrochemical performances of the Li-rich cathodes with different amounts of $LiNi_{0.5}Mn_{1.5}O_4$ (5, 10, and 20 wt %) coating are investigated. It is demonstrated that the coating samples exhibit superior rate capability and cycling stability than the bare sample. Particularly, the 20 wt % coated sample delivers a Li storage capacity of 170.7 mAh g^{-1} with a capacity retention of 94.4% in 100 cycles at a high rate of 5 C (1250 mA g^{-1}), showing a prospect for practical lithium-ion battery applications. More significantly, the synthetic method proposed in this work is facile and low-cost and possibly could be adopted for large-scale production of surface-modified cathode materials.

AUTHOR INFORMATION

Corresponding Authors

*Tel.:+86-731-84576404. Fax: +86-731-84576404. E-mail: zxchen@hnu.edu.cn.

*Tel.:+86-731-84573149. Fax: +86-731-84573149. E-mail: zhengchunman@hotmail.com.

Notes

The authors declare no competing financial interest.

ACKNOWLEDGMENTS

The authors thank the financial support from program of science and technology innovative research team in higher education institutions of Hunan province and the National Science Foundation of China (201303262) and Hunan Provincial Natural Science Foundation of China (13jj4004).

REFERENCES

(1) Sun, Y.-K.; Chen, Z.; Noh, H.-J.; Lee, D.-J.; Jung, H.-G.; Ren, Y.; Wang, S.; Yoon, C. S.; Myung, S.-T.; Amine, K. Nanostructured High-Energy Cathode Materials for Advanced Lithium Batteries. *Nat. Mater.* **2012**, *11*, 942−947.

(2) Xiao, J.; Chen, X.; Sushko, P. V.; Sushko, M. L.; Kovarik, L.; Feng, J.; Deng, Z.; Zheng, J.; Graff, G. L.; Nie, Z.; Choi, D.; Liu, J.; Zhang, J.-G.; Whittingham, M. S. High-Performance $LiNi_{0.5}Mn_{1.5}O_4$ Spinel Controlled by Mn^{3+} Concentration and Site Disorder. *Adv. Mater.* **2012**, *24*, 2109−2116.

(3) Chen, Z.; Qiu, S.; Cao, Y.; Ai, X.; Xie, K.; Hong, X.; Yang, H. Surface-Oriented and Nanoflake-Stacked $LiNi_{0.5}Mn_{1.5}O_4$ Spinel for High-Rate and Long-Cycle-Life Lithium Ion Batteries. *J. Mater. Chem.* **2012**, *22*, 17768−17772.

(4) Chen, Z.; Qiu, S.; Cao, Y.; Qian, J.; Ai, X.; Xie, K.; Hong, X.; Yang, H. Hierarchical Porous Li_2FeSiO_4/C Composite with 2 Li Storage Capacity and Long Cycle Stability for Advanced Li-Ion Batteries. *J. Mater. Chem. A* **2013**, *1*, 4988−4992.

(5) Thackeray, M. M.; Kang, S.-H.; Johnson, C. S.; Vaughey, J. T.; Benedek, R.; Hackney, S. A. Li_2MnO_3-Stabilized $LiMO_2$ (M = Mn, Ni, Co) Electrodes for Lithium-Ion Batteries. *J. Mater. Chem.* **2007**, *17*, 3112−3125.

(6) Armstrong, A. R.; Holzapfel, M.; Novak, P.; Johnson, C. S.; Kang, S. H.; Thackeray, M. M.; Bruce, P. G. Demonstrating Oxygen Loss and Associated Structural Reorganization in the Lithium Battery Cathode $Li[Ni_{0.2}Li_{0.2}Mn_{0.6}]O_2$. *J. Am. Chem. Soc.* **2006**, *128*, 8694−8698.

(7) Yabuuchi, N.; Yoshii, K.; Myung, S.-T.; Nakai, I.; Komaba, S. Detailed Studies of a High-Capacity Electrode Material for Rechargeable Batteries, Li_2MnO_3−$LiCo_{1/3}Ni_{1/3}Mn_{1/3}O_2$. *J. Am. Chem. Soc.* **2011**, *133*, 4404−4419.

(8) Croy, J. R.; Kim, D.; Balasubramanian, M.; Gallagher, K.; Kang, S.-H.; Thackeray, M. M. Countering the Voltage Decay in High Capacity $xLi_2MnO_3{\cdot}(1-x)LiMO_2$ Electrodes (M = Mn, Ni, Co) for Li^+-Ion Batteries. *J. Electrochem. Soc.* **2012**, *15*, A781−A790.

(9) Jiao, L. F.; Zhang, M.; Yuan, H. T.; Zhao, M.; Guo, J.; Wang, W.; Zhou, X. D.; Wang, Y. M. Effect of Cr Doping on the Structural, Electrochemical Properties of $Li[Li_{0.2}Ni_{0.2-x/2}Mn_{0.6-x/2}Cr_x]O_2$ (x = 0, 0.02, 0.04, 0.06, 0.08) as Cathode Materials for Lithium Secondary Batteries. *J. Power Sources* **2007**, *167*, 178−184.

(10) Qiu, S.; Chen, Z.; Pei, F.; Wu, F.; Wu, Y.; Ai, X.; Yang, H.; Cao, Y. Synthesis of Monoclinic $Li[Li_{0.2}Mn_{0.54}Ni_{0.13}Co_{0.13}]O_2$ Nanoparticles by a Layered-Template Route for High-Performance Li-Ion Batteries. *Eur. J. Inorg. Chem.* **2013**, *2013*, 2887−2892.

(11) Wang, D.; Belharouak, I.; Zhou, G.; Amine, K. Nanoarchitecture Multi-Structural Cathode Materials for High Capacity Lithium Batteries. *Adv. Funct. Mater.* **2013**, *23*, 1070−1075.

(12) Wei, G.-Z.; Lu, X.; Ke, F.-S.; Huang, L.; Li, J.-T.; Wang, Z.-X.; Zhou, Z.-Y.; Sun, S.-G. Crystal Habit-Tuned Nanoplate Material of $Li[Li_{1/3-2x/3}Ni_xMn_{2/3-x/3}]O_2$ for High-Rate Performance Lithium-Ion Batteries. *Adv. Mater.* **2010**, *2*, 4364−4367.

(13) Jiang, K.-C.; Wu, X.-L.; Yin, Y.-X.; Lee, J.-S.; Kim, J.; Guo, Y.-G. Superior Hybrid Cathode Material Containing Lithium-Excess Layered Material and Graphene for Lithium-Ion Batteries. *ACS Appl. Mater. Interfaces* **2012**, *4*, 4858−4863.

(14) Min, J. W.; Yim, C. J.; Im, W. B. Facile Synthesis of Electrospun $Li_{1.2}Ni_{0.17}Co_{0.17}Mn_{0.5}O_2$ Nanofiber and Its Enhanced High-Rate Performance for Lithium-Ion Battery Applications. *ACS Appl. Mater. Interfaces* **2013**, *5*, 7765−7769.

(15) He, W.; Qian, J.; Cao, Y.; Ai, X.; Yang, H. Improved Electrochemical Performances of Nanocrystalline $Li[Li_{0.2}Mn_{0.54}Ni_{0.13}Co_{0.13}]O_2$ Cathode Material for Li-Ion Batteries. *RSC Adv.* **2012**, *2*, 3423−3429.

(16) Li, G. R.; Feng, X.; Ding, Y.; Ye, S. H.; Gao, X. P. AlF_3-Coated $Li(Li_{0.17}Ni_{0.25}Mn_{0.58})O_2$ as Cathode Material for Li-Ion Batteries. *Electrochim. Acta* **2012**, *78*, 308−315.

(17) Noh, J.-K.; Kim, S.; Kim, H.; Choi, W.; Chang, W.; Byun, D.; Cho, B.-W.; Chung, K. Y. Mechanochemical Synthesis of Li_2MnO_3 Shell/$LiMO_2$ (M = Ni, Co, Mn) Core-Structured Nanocomposites for Lithium-Ion Batteries. *Sci. Rep.* **2014**, *4*, DOI:10.1038/srep04847.

(18) Song, B.; Liu, H.; Liu, Z.; Xiao, P.; Lai, M. O.; Lu, L. High Rate Capability Caused by Surface Cubic Spinels in Li-Rich Layer-Structured Cathodes for Li-Ion Batteries. *Sci. Rep.* **2013**, *3*, DOI:10.1038/srep03094.

(19) Fu, Q.; Du, F.; Bian, X.; Wang, Y.; Yan, X.; Zhang, Y.; Zhu, K.; Chen, G.; Wang, C.; Wei, Y. Electrochemical Performance and Thermal Stability of $Li_{1.18}Co_{0.15}Ni_{0.15}Mn_{0.52}O_2$ Surface Coated with the Ionic Conductor Li_3VO_4. *J. Mater. Chem. A* **2014**, *2*, 7555−7562.

(20) Guo, S.; Yu, H.; Liu, P.; Liu, X.; Li, D.; Chen, M.; Ishida, M.; Zhou, H. Surface Coating of Lithium-Manganese-Rich Layered Oxides with Delaminated MnO_2 Nanosheets as Cathode Materials for Li-Ion Batteries. *J. Mater. Chem. A* **2014**, *2*, 4422−4428.

(21) Qiao, Q. Q.; Zhang, H. Z.; Li, G. R.; Ye, S. H.; Wang, C. W.; Gao, X. P. Surface Modification of Li-Rich Layered $Li(Li_{0.17}Ni_{0.25}Mn_{0.58})O_2$ Oxide with Li-Mn-PO_4 as the Cathode for Lithium-Ion Batteries. *J. Mater. Chem. A* **2013**, *1*, 5262−5268.

(22) Wu, F.; Li, N.; Su, Y.; Shou, H.; Bao, L.; Yang, W.; Zhang, L.; An, R.; Chen, S. Spinel/Layered Heterostructured Cathode Material for High-Capacity and High-Rate Li-Ion Batteries. *Adv. Mater.* **2013**, *25*, 3722−3726.

(23) Croy, J. R.; Gallagher, K. G.; Balasubramanian, M.; Chen, Z.; Ren, Y.; Kim, D.; Kang, S.-H.; Dees, D. W.; Thackeray, M. M. Examining Hysteresis in Composite $xLi_2MnO_3{\cdot}(1-x)LiMO_2$ Cathode Structures. *J. Phys. Chem. C* **2013**, *117*, 6525−6536.

(24) Gu, M.; Genc, A.; Belharouak, I.; Wang, D.; Amine, K.; Thevuthasan, S.; Baer, D. R.; Zhang, J.-G.; Browning, N. D.; Liu, J.; Wang, C. Nanoscale Phase Separation, Cation Ordering, and Surface Chemistry in Pristine $Li_{1.2}Ni_{0.2}Mn_{0.6}O_2$ for Li-Ion Batteries. *Chem. Mater.* **2013**, *25*, 2319−2326.

(25) Chen, Y.; Chen, Z.; Xie, K. Effect of Annealing on the First-Cycle Performance and Reversible Capabilities of Lithium-Rich Layered Oxide Cathodes. *J. Phys. Chem. C* **2014**, *118*, 11505−11511.

(26) Lee, J.; Urban, A.; Li, X.; Su, D.; Hautier, G.; Ceder, G. Unlocking the Potential of Cation-Disordered Oxides for Rechargeable Lithium Batteries. *Science* **2014**, *34*, 519−522.

(27) Wang, Q. Y.; Liu, J.; Murugan, A. V.; Manthiram, A. High Capacity Double-Layer Surface Modified $Li[Li_{0.2}Mn_{0.54}Ni_{0.13}Co_{0.13}]O_2$ Cathode with Improved Rate Capability. *J. Mater. Chem.* **2009**, *19*, 4965−4972.

(28) Lee, E.-S.; Huq, A.; Chang, H.-Y.; Manthiram, A. High-Voltage, High-Energy Layered-Spinel Composite Cathodes with Superior Cycle Life for Lithium-Ion Batteries. *Chem. Mater.* **2012**, *24*, 600−612.

(29) Wu, F.; Li, N.; Su, Y.; Zhang, L.; Bao, L.; Wang, J.; Chen, L.; Zheng, Y.; Dai, L.; Peng, J.; Chen, S. Ultrathin Spinel Membrane-Encapsulated Layered Lithium-Rich Cathode Material for Advanced Li-Ion Batteries. *Nano Lett.* **2014**, *14*, 3550−3555.

(30) Jiang, M.; Key, B.; Meng, Y. S.; Grey, C. P. Electrochemical and Structural Study of the Layered, "Li-Excess" Lithium-Ion Battery Electrode Material $Li[Li_{1/9}Ni_{1/3}Mn_{5/9}]O_2$. *Chem. Mater.* **2009**, *21*, 2733−2745.

(31) Robertson, A. D.; Bruce, P. G. Mechanism of Electrochemical Activity in Li_2MnO_3. *Chem. Mater.* **2003**, *15*, 1984−1992.